Ewing's sarcoma in a fourth century AD urban cemetery of northern Gaul

Joël Blondiaux, Eric Binet, Pierre Marchandise, Xavier Demondion, Thomas Colard

Ewing's sarcoma in a fourth century AD urban cemetery of northern Gaul

Joel Blondiaux a, *, Eric Binet b, Pierre Marchandise c, Xavier Demondion a, d, Thomas Colard a, e.

[a]Centre dõEtudes Paléopathologiques du Nord, 36 rue Jules Ferry, 59127 Walincourt-Selvigny, France

[b]Service Archéologie Préventive, Amiens-Métropole, BP 2720, 80027 Amiens Cedex 1, France

[c]EA 4490 PMOI Physiopathologie des Maladies Osseuses et Inflammatoires . Faculté de Chirurgie dentaire ; Place de Verdun, 59000 Lille France. Pierre.marchandise@univ-lille2.fr

[d]Service dõImagerie Ostéo-articulaire, Hôpital Salengro 59037 Lille Cedex France

[e] Lille University, Forensic Taphonomy Unit ï Anthropology, Lille Forensic Institute, 59000, France

Abstract:

There are only four reports of the occurrence of primary or secondary bone tumors evoking Ewing's sarcoma (ES) in skeletal material provided by archeology. We report here the imaging results of a case confirming, for the first time in paleopathology, the diagnosis of ES, malignant tumor of childhood and young adults which brings together 17% of bone sarcoma today. The observation combined the signature of the primary tumor in a right rib fragment and a secondary location in a first sternebra. The micro-CT scan, in this particular case, avoids the use of light and electron microscopy to establish the diagnosis of Ewing's tumor. A taphonomic change of the right rib cage, observed at the time of excavation, is a supplementary confirmation of the diagnosis.

Introduction:

James Ewing, a New York pathologist, first described in 1921 a " bone diffuse endothelioma", later called Ewing sarcoma (ES). Since its publication, numerous theories have been proposed about the origin of Ewing sarcoma (Hadju 2006). It is still not definitively known. The two most current assumptions suggest that this tumor arises from a primitive cell either an embryonic stem cell or a pluripotent mesenchymal cell . Pathologists have long known that Ewing's sarcoma is similar to a soft tissue tumor called primitive neuroectodermal tumor (PNET) , that one being even rarer. When the tumor affects the skeleton and is originating from bone, it is called ES. When the lesion is originating from soft tissue, it is called PNET. In the early 1980s, ES and PNET were found not only identical when viewed under the microscope, but they also share, in over 95% of cases, a chromosomal abnormality called translocation (Aurias 1984). Since then, both tumors were grouped into a single class entitled Ewing Sarcoma family Tumors (ESFT) because of this common translocation (Kerst et al 2001). In ESFT, translocation is between chromosomes 11 and 22 and is designated by t (11; 22).

The ESFT are very rare and occur with a prevalence of just one for 3 million people aged less than 20 years. In 90% of cases, ESFT occur in patients between 5 and 25 years. After 25 years, they are extremely rare. About 25% of cases occur before 10 years, while 65% occur in the second decade. Approximately 10% of patients are older than 20 years at diagnosis. Males are affected more often than females (6: 1). The pelvis is the most common location, followed in order by the femur, tibia, humerus, scapula and rib. However, ESFT can be found in all parts of anatomy. They are nine times more common in Caucasians than in African Americans (Helms 1989).

Among primary tumors of bone affecting the chest, as it is in the present case , which are themselves very rare, the most common is chondrosarcoma, followed by sarcomas (osteosarcoma and ESFT) , then by multiple myeloma and lymphomas (Henk et al. 1998). The chest wall may also be invaded by extension from a lung carcinoma and metastases of extra-thoracic cancers. Imaging plays an important role in the diagnosis of tumors involving the whole bony skeleton. Our objective here is to examine the imaging characteristics of neoplasms affecting the skeleton of the chest wall. On plain radiographs, the ESFT appear lytic lesions around density formations or mixed formations and rarely as a single sclerotic lesion . They are located primarily in the diaphyseal and metadiaphyseal parts of long bones of the lower extremities, but the ESFT of rib cage are associated with a very homogeneous massive tumor extended to soft tissue and usually developing as solitary lesion centered on rib, sternum, scapula, clavicle or paravertebral regions. Metastasis spread to lungs, bones, bone marrow, liver and brain.

Preceding this presentation, the paleopathological literature has little called the diagnosis of ESFT, which may sound normal given its current prevalence and age occurrence. Among the previous four presumptive paleopathological descriptions of ESFT, one is located on a femur (Suzuki 1987) and the other three are presumed to be metastatic and located on pelvis (Ruffer 1921), skull (Campillo et al. 1977, 1984), and in the distal end of a fractured ulna (Löwen, 1998). In 2008, Brothwell retained none of these cases as ES when he supported the likelihood of many other types of osteosarcoma in the paleopathological literature. It is in any case certain that none of these descriptions, except perhaps that of Löwen (1998) carry conviction, this may be also because in none of these cases exhaustive imaging or microscopy have been convened and the only microscopy made by Campillo (1984) is clearly not confirmatory.

Material:

The skeleton of which we propose the paleopathological study was excavated from the site of Amiens Caserne Dejean by E. Binet in 2012 (Fig. 1). The results of the bio-archaeological study of the Amiens Caserne Dejean site brought interest in the contrasting aspects of urban cemeteries used by different social and economic sectors of the Samarobriva metropolis during the fourth century AD. In this cemetery, a traditional, sedentary, peaceful society, somewhat hierarchical, enjoyed good living conditions and a satisfactory survivorship for the time. The frequency of burial looting suggested by five perforations of bones (probes holes) revealed a relative material comfort guaranteeing the deposit of precious objects offered secondarily to the lust of the graveyard robbers and ultimately leading to increased degradation or disappearance of skeletons. 185 burials were excavated, Half of them (92) were empty of bones and conservation index is particularly low; the immature skeletons represent only 17 % of skeletons determinable for age. Burial 140 was located in the northwest part of the cemetery (Fig. 2). The skeleton was supine, bent and upper limbs folded

on the abdomen. He was like most of the other graves NO oriented (head) / SE (305 °). The skeleton is undisturbed and well represented. It rests supine on the pit bottom. The skull is partially leveled but post mortem fractures and displacement of certain fragments indicate that it collapsed on itself. Its original position appears to be antero-superior, the crushing of the burial occasioning a rear toggle effect on the half back. The mandible is disconnected and based on the left clavicle. The spine is relatively complete and shows no particular movement.

The rib cage is flat, the hemi-thorax having an opening such as right ribs abut against the right humerus (Figure 3).

The humeri are on the opposite side appearance. The forearms are semi-flexed on the abdomen, the left passes over the right. The hands rest in the dorsal iliac wings, the right is slightly dislocated. The pelvis is open but a light volume is retained by effect of lateral forces.

The lower limbs are extended; the femurs are in frontal antero-medial appearance. The right patella is in anatomical position. Lateral rotation is more pronounced for the right femur. Tibias are facing antero-medial appearance. The right foot was rejected loose on the left foot, apparently displaced during installation of a modern structure. The effects of stress on the arms and coxal and flatness up the chest indicate an empty space and a non restricted decomposition. The alignments of nails, sometimes in direct proximity of the skeleton, also demonstrate the use of a coffin.

Figure 1 Location of Amiens et Amiens Caserne Dejean site in Northern France

Figure 2 Map of Caserne Dejean site and location of burial S140 (black arrow)

Figure 3 Burial S 140 .

Methods:

In addition to the macroscopic description, we used the standard X-ray, CT-scan and Micro CT scan.

Observation:

The incomplete skeleton is fairly well represented (Fig.4) but poorly preserved after careful cleansing (CI 65%). This is a male individual (robustness, mandible and size), rather young (tooth wear and bone density). Cementochronological age of tooth 24 is 26 years. One notices lumbar Schmorl nods in L3 and L4 plateaus and l lower plateaus of L1 and L2.

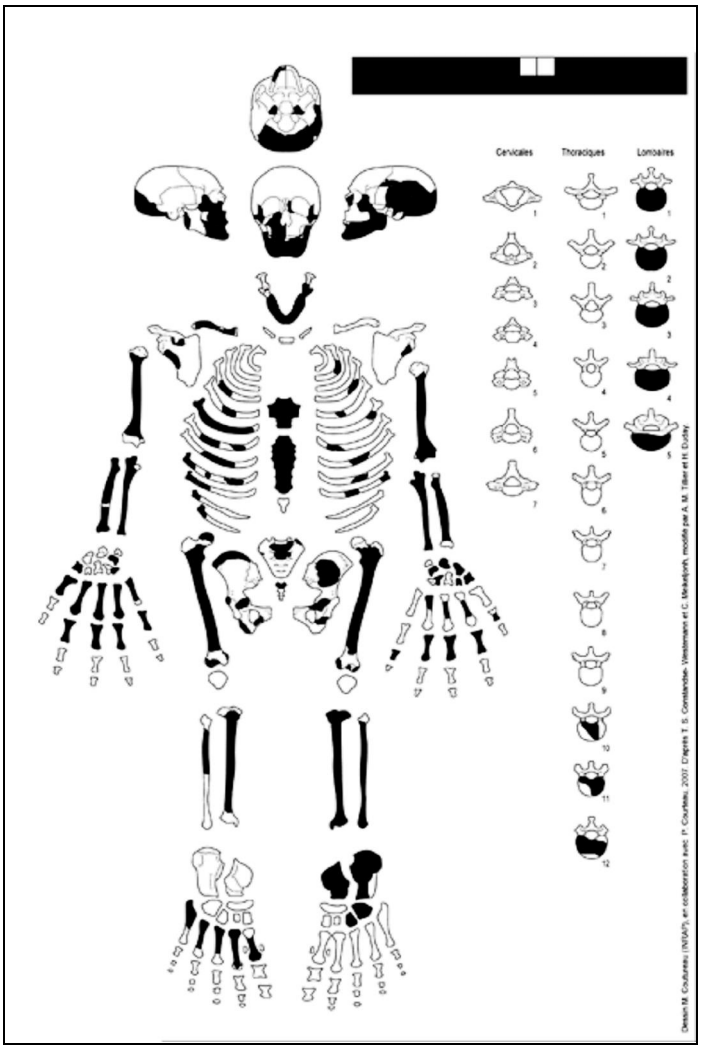

Figure 4 Conservation file of the Amiens Caserne Dejean 140 skeleton. In black, preserved bone and yeeth.

S 140 individual exhibited two lesions, one on the side of the first endothoracic sternebra, the other on a right costal fragment.

The rib arch is interrupted in the middle of the body and the front end combines eroded and thick periosteal appositions on the intrathoracic and exothoracic surfaces over a length of about 20 mm with a remodeling and hypervascular appearance of the bone around the end of the rib fragment (Fig. 6 & 7). The distal surface of the bone is also remodeled and draws a trabecular bone depression on the lateral side while the trabeculae are thickened on the visceral side and the appositions merge on to the partial destruction of the cortical bone. The X-Ray (Fig.7) discovers a cortical uprising aspect separated by a laminated space appearing as a triangular lesion placed on the pleural surface at the end of the bone. The more radiolucent triangular formation at its center based on cortical thickening which is blurred and is also associated with a trabecular thickening on contact.

Figure 5 ACD 140. Right rib, lateral view.

Figure 6 ACD 140 : Right rib , remodeling of the anterior extremity of the fragment.

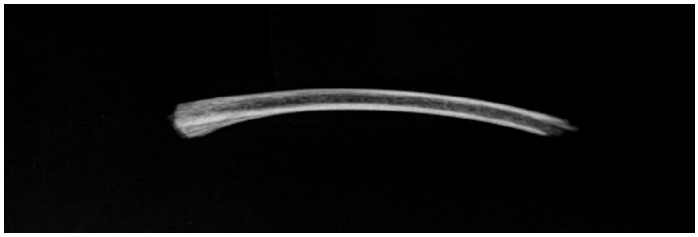

Figure 7 ACD 140. Right rib : Xray

A rounded proliferative lesions, the size of a large pea, seats in the middle on the endothoracic surface of the first sternebra (Fig.8). It measures 13 mm in diameter and 6 mm in height. The appearance is that of thickened trabecular bone merging from a depression of the bone surface. X-Ray (Fig. 9) and CT-scan confirmed a protruding extensive dense mass in the body of the sternebra within a zone of radiolucent area, breaking the cortical and blurring its sharpness In addition, trabecular thickening resembles that of the rib.
The micro-CT scan of both bone pieces extends the specific aspects of the densed newly formed bone with destructive peripheral areas and some areas of terrestrial deposits at the bottom of a tunneled destructive zone in the sternum.

Figure 8 ACD 140. Sternum, endothoracic view, protruding lesion in the first sternebra.

Figure 9 ACD 140. Sternum, Xray, front and profile.

The micro-CT of the rib end (Figure 10) specifies the destructive effects of the tumor on the cortical bone on both the distal portion and the visceral surface of the bone with deep lacunae thqt may correspond to an osteolytic front; They contrast with the laminated sparse appositions over the cortical bone and appositions of trabeculae adjacent to the cortical bone.

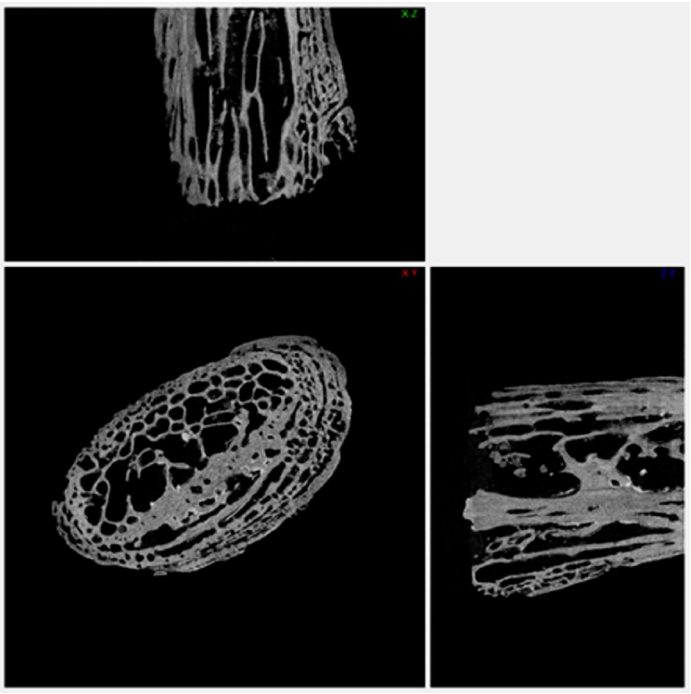

Figure 10 ACD 140; right rib Micro-CT scan: up transversal section, bottom-left lateral section and bottom-right sagittal section.

The micro-CT scan of the sternum (Fig. 11 & 12) describes perfectly the two aspects of the central tumor combining extensive destruction, in the center of what seats a dense mass of thick trabeculae which breaks and extends beyond the ventral cortical bone. An empty space at the right of the tumor mass has allowed circumscribed accumulation of compact and well-defined terrestrial deposits distinguishable from the newly formed bone mass.

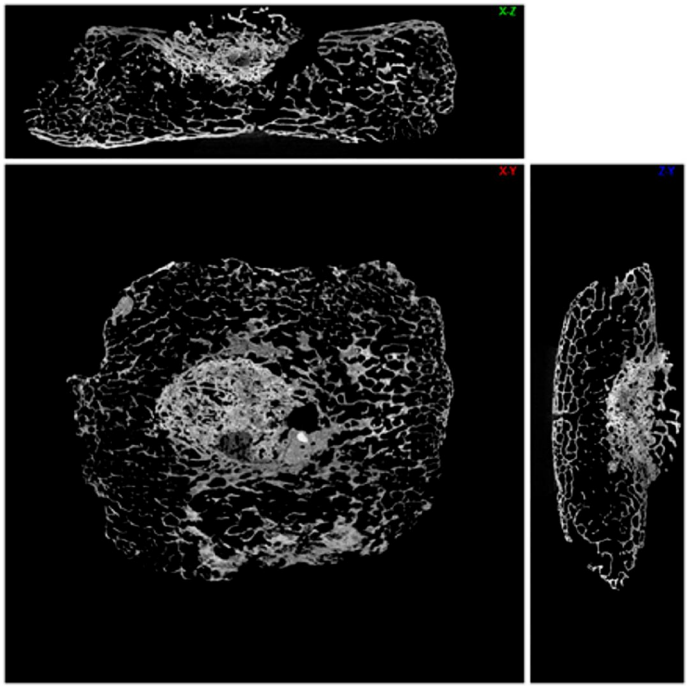

Figure11 ACD 140; first sternebra, Micro-CT scan: up sagittal section; bottom left frontal section; bottom-right transversal section.

Discussion:

If it were not for the large erosions, the costal remodeling would think of a recent fracture callus of approximately 15 days (Blondiaux 2000 de Boer 2013, 2014); the absence of the opposite distal end as the macroscopic aspects are not typical callus recent fracture, due to the paradoxical cortical remodeling and thickening of trabecular bone adjacent to the destructed cortical zone of the bone.

Imaging, both by the location and the general appearance, eliminate also an infectious origin (osteomyelitis), a chondrosarcoma, essentially constructive or a multiple myeloma, essentially destructive. The laminated aspect of the costal lesion and the discontinuous aspect of periosteal reaction, signs of the fast activity of the tumor process, type III according to Chhem RK et al (2008) are in favor of an ESFT while the destruction of cortical bone, appositions and peripheral trabecular erosion are in favor of an osteosarcoma or an ES secondary location. ESFT are found mainly in male (60%) and young individuals (90% between 5 and 30 years) and represents 10% of primary tumors of bone. Helms (1989) noted that in patients over 25 years, the flat bones are most frequently affected. The symptomatology is that of local tumors accompanied by pain, fever, weight loss, anemia, mimicking an infectious syndrome. Main locations are the bones of the lower extremities, the femur (22%), the ilium (12%), the tibia (11%), the humerus (10%), the fibula (9%) and the ribs (8%). The prognosis as most sarcomas is appalling without treatment of radiotherapy, chemotherapy or surgery. ES is a highly invasive tumor, locally and remotely through blood; The tumor mass is much greater than the bone lesion itself and we have indirect evidence with the taphonomy (Fig. 4) that shows an open chest accentuated on the right side and a suggestive displacement of the ribs following the intra thoracic expansion of an ES. In continuation of this rib lesion a large tumor mass invading the chest cavity must have proliferated (Shamberger et al. 2001), probable and ultimate cause of death of this young adult. Eventually, taphonomy confirms the proliferations often associated with pleurisy and explains the horizontal fall of the ribs against the right humerus compared to the natural vertical one on the left side at distance of the left humerus.

The sternal location, equally by its eloquent dense aspects, well differentiated by the micro-CT from post mortem deposits and by a large destructive zone, probably corresponds to a locoregional metastasis of the rib primary tumor. 15 to 30% of the individuals with this tumor have a metastatic form. The locoregional development of new tumors occurs in 21-25% of ESFT. (Resnick et al 1995).

Conclusion

Burial S 140 excavated from the Late Antiquity cemetery of Amiens Caserne Dejean, documents a rare but not so exceptional neoplasia, a Ewing's sarcoma or ESFT. Imagery and in particular the micro-CT scan, retrieve the architecture and the local development of the rib primary tumor, with destructive and constructive aspects (Codman triangle), as well as the locoregional extension in the sternum with cortical and trabecular destruction and dense and thickened trabeculae of the tumor core. Taphonomy of the rib cage explains the displacement of the right ribs since the large intrathoracic volume of the tumor and probable associated pleurisy developed from one side; a paleoproteomic analysis could be a continuation of this

research, as to find the ESFT marker protein produced by the chromosomal translocation t (11,12) which is always associated with them.

References

Aurias A, Rimbaut C, Buffe D, Zucker JM, Mazabraud A. 1984 Translocation involving chromosome 22 in Ewing's sarcoma. A cytogenetic study of four fresh tumors. Cancer Genet Cytogenet. 12,1,21-25.

Blondiaux J. 2000. The ageing of fracture healing in paleopathology with light microscopic observation. Abstracts of the 13th European meeting of the Paleopathology Association. Chieti, Italy.

Brothwell Don 2008. Tumours and tumour-like processes in Ron Pinhasi and Simon Mayx eds : Advances in human palaeopathology. Wiley ed. 253-281

Campillo D 1977 Paleopathologia des craneo en Cataluna, Valencia y Baleares . Montblanc-Marin ed. 630 pages.

Campillo D., Mar-Barcells V. J. 1984. Microscopy of osteal tumors in paleopathology. In Proceedings of the Vth European meeting of the Paleopathology Association (Siena) 35-43.

Chhem R. K, Saab G., Brothwell D. R. 2008. Diagnostic paleoradiology for paleopathologists. In R.K. Chhem, D.R. Brothwell: Paleoradiology, imaging mummies and fossils . Springer 73-118.

de Boer H. H. 2014 Dry bone Histology, technicalities, diagnostic value and new applications. PhD dissertation University of Leiden . 203 pages.

De Boer H. H., Van der Merwe A. E., Maat G. J. R. 2013. Survival time after fracture or amputation in a 19th century mining population at Kimberly, South Africa. In: South Efrican Archaeological Society, Goodwin Series 11: Skeletal identity of Southern African p opulations; lessons from outside South Africa. Steyn M., Morris A. G., Maat G. J. R. , Morongwa N. M. (Eds.), 52-60.

Ewing J. 1921: Diffuse endothelioma of bone, Proc NY Pathol Soc. 21:17.

Hajdu S. I. 2006 A Note from History: The Enigma of Ewingôs Sarcoma Annals of Clinical & Laboratory Science, vol. 36, no. 1,

Helms A. 1989. Fundamentals of skeletal radiology. W.B. Saunders, Philadelphia;

Henk CB, Grampp S, Weisbauer P, Zoubek A, Kainberger F, Breitensel M. 1998 Ewing sarcoma. Diagnostic Imaging. Radiologie 38, 509-522.

Kerst JM, Van Coevorden F, Peterse J, Haas RL, Linn SC. 2004. Young adults with Ewingôs sarcoma Ned Tijdschr Geneeskd 148, 1355-1358.

Löwen, Holger 1994 A Ewing Sarcoma from an Early Medieval Hillside in Westphalia. [Abstract]. HOMO 45(Supplement, Special Issue, Xth European Meeting of the Paleopathology Association, Göttingen, Germany, 29 August©3 September 1994):S77.

Löwen, Holger 1994 A Ewing's Sarcoma from an Early Medieval Hillside in Westphalia. [Abstract]. In: Eve Cockburn, ed. Papers on Paleopathology Presented at the Tenth European Members Meeting of the Paleopathology Association, Göttingen, Germany, 29 August©3 September 1994, p. 15.

Löwen H. 1998 A Ewingôs sarcoma from an early medieval hillside in Westphalia . Journal of Palaeopathology 10, 3 , 127-132.

Resnick D. 1995 Diagnosis of bone and Joint diseases. W. B. Saunders Company

Ridings, G. R. 1964 Ewing's Tumor. Radiologic Clinics of North America

2(2):315-325

Ruffer M. A. 1921 Studies in the palaeopathology of Egypt. The University og Chicago Press .

Shamberger RC, Grier HE. 2001. Ewingôs sarcoma/primitive neuroectodermal tumor of the chest. Semin. Pediatr. Surg. 10,153-160.

Sherman, Robert S., and Kenneth Y. Soong 1956 Ewing's Sarcoma: Its Roentgen Classification and Diagnosis. Radiology 66(4):529-539.

Suzuki T. 1987. Paleopathological study of a case of osteosarcoma. AJPA 74, 3 309-318/